A Linear Kalman Notch Filter for Power-Line Interference Cancellation

Reza Sameni
School of Electrical & Computer Engineering
Shiraz University
Shiraz, Iran
rsameni@shirazu.ac.ir

***Abstract*—A discrete-time linear Kalman filter is presented for removing power-line interference from biomedical recordings. The theoretical aspects of this filter, the relationship with conventional digital IIR and adaptive IIR notch filters, and its steady state behavior are studied in detail. As compared to previous studies, the filter is linear and does not require any information about the amplitude nor the phase of the power-line interference. The proposed method is fairly general and is applicable to broad classes of signals contaminated by periodic noise. The proposed model also accounts for multiple harmonics. Two examples of its applications for electrocardiogram and electroencephalogram denoising are presented.**

***Index Terms*—Kalman Filter, Power-line Interference Cancellation, Notch Filter**

I. Introduction

Power-line interference (PLI) is an inevitable interference in biosignal measurement systems. Due to the importance of removing these interferences, the domain is fairly mature. The classical approach for removing PLI is to use a (IIR) notch filter with the notch frequency located at the PLI frequency [1]. However, high quality-factor (Q-factor) notch filters are difficult to design, they are susceptible to noise and may easily become instable. Therefore, it is desirable to have adaptive notch filters that somehow adapt their frequency selectivity according to the signal/noise contents of the measured signals. To date, various adaptive notch filters have been proposed in the literature [2], [3], [1], [4], [5]. The intuition behind these filters is to adaptively manipulate the Q-factor of the filter [6] (cf. [3] eq. (10)).

More recently, some researchers have used Extended Kalman Filters (EKF) for PLI tracking and cancellation [7], [8], [9], [10]. These studies have considered the possibility of power-line frequency deviations and tracking, which are important issues in power systems. However, according to power system quality standards, the frequency deviation of the PLI is of the order of ± 0.01Hz [11, Ch. 23]. Therefore, for biosignal processing applications, the PLI frequency deviation is practically negligible. On the other hand, in such applications, the knowledge of PLI amplitude (and phase) is more limiting and important; since the amplitude of the PLI induced over the desired biosignals can easily change with the sensor configuration, patient positioning, and impedance changes of the body volume conductor. It is therefore, desirable to have an adaptive filter that does not require the knowledge of the PLI amplitude and phase.

Despite the rich literature in this field, to the author's knowledge, discrete-time linear Kalman Filters (KF) have not been used for PLI cancellation. In this work, we develop a rather simple and totally linear KF for PLI cancellation. The major contribution of this study is the theoretical study of this linear framework and its relationship with classical second-order adaptive notch filters [2], [3].

In this study, no assumptions are made about the possible dynamics of the biosignals contaminated by PLI. However, if prior information is available about the dynamics of the contaminated signals (cf. [12], [13], [14]), the hereby presented dynamical models can be simply augmented with them, to form a more general framework for biosignal denoising. It is further shown that the method can be extended to PLI having more than one harmonics.

The rest of the paper is organized as follows: in Section II the proposed model is developed. Theoretical issues regarding the stability, convergence, steady-state behavior, implementation issues and its extension to multiple harmonics are presented in Sections III to VI. Two case studies are presented in Section VII for electrocardiogram and electroencephalogram denoising, and the last section is devoted to some concluding remarks.

II. Method

Discrete-time single tone power-line interference may be considered as a sinusoid with an arbitrary amplitude and phase:

$$x_n = B\cos(\omega_0 n + \phi), \tag{1}$$

where $\omega_0 = 2\pi f_0/f_s$, n is the time index, and f_0 and f_s are the PLI and sampling frequencies, respectively. Using basic trigonometric identities, x_n can be recursively computed as follows:

$$x_{n+1} + x_{n-1} = 2\cos(\omega_0)x_n \tag{2}$$

A more conservative form of this model, which is more suitable for a KF, is to consider an additive zero-mean random term w_n, to represent the possible model errors, including minor amplitude, phase, or frequency deviations. The modified dynamic model is

$$x_{n+1} + x_{n-1} = 2\cos(\omega_0)x_n + w_n \tag{3}$$

978-1-4673-1479-4/12/$31.00 ©2012 IEEE

Although phase and frequency errors are not additive, since the PLI is practically rather stationary and does not have rapid deviations, it is shown that this simplified model works very well in practice. In fact, in Kalman filter engineering, it is common practice to enter stochastic terms (even in fully deterministic models), to make the filter more flexible.

Biosignals contaminated by PLI can be considered as superposition of the PLI and the desired biosignals, plus other undesired signal/noise, i.e.,

$$y_n = x_n + v_n, \tag{4}$$

where x_n is the PLI and v_n is a zero-mean random term, representing all non-PLI signals and noises[1]. In this study, we have neglected the fact that v_n, which is a combination of biosignals and noises, may itself be represented by a dynamical model. The incorporation of such dynamics can generally improve the hereby presented results, as suggested in [12], [13], [14].

In order to construct a KF for estimating and removing the PLI, the dynamic equation in (3) needs to be converted to a state-space form. There are several standard methods for representing a dynamic model in state-space form, which are known as *canonical representations*. Two of the most common canonical representations, which are of great importance in control theory, are the *controllable* and *observable* canonical forms [15]. The resulting models of these forms are guaranteed to be *controllable* and *observable*, respectively [2]. Based on these concepts, (3) and (4) can be rewritten as follows:

$$\begin{cases} \mathbf{x}_{n+1} = A\mathbf{x}_n + \mathbf{b}w_n \\ y_n = \mathbf{h}^T\mathbf{x}_n + v_n \end{cases} \tag{5}$$

where $\mathbf{x}_n \doteq [x_n \quad x_{n-1}]^T$, $A \doteq \begin{bmatrix} 2\cos(\omega_0) & -1 \\ 1 & 0 \end{bmatrix}$, $\mathbf{b} \doteq [1 \quad 0]^T$, and $\mathbf{h} \doteq [1 \quad 0]^T$.

The dynamical model is now complete and may be applied to noisy biosignals using classical iterative KF equations:

1) *Time propagation*:

$$\begin{aligned} \hat{\mathbf{x}}_{n+1}^- &= A\hat{\mathbf{x}}_n^+ \\ P_{n+1}^- &= AP_n^+A^T + q_n\mathbf{b}\mathbf{b}^T \end{aligned} \tag{6}$$

2) *Kalman gain*:

$$\mathbf{K}_n = \frac{P_n^-\mathbf{h}}{\mathbf{h}^TP_n^-\mathbf{h} + r_n} \tag{7}$$

3) *Measurement propagation*:

$$\begin{aligned} \hat{\mathbf{x}}_n^+ &= \hat{\mathbf{x}}_n^- + \mathbf{K}_n[y_n - \mathbf{h}^T\hat{\mathbf{x}}_n^-] \\ P_n^+ &= P_n^- - \mathbf{K}_n\mathbf{h}^TP_n^- \end{aligned} \tag{8}$$

where $q_n \doteq E\{w_n^2\}$, $r_n \doteq E\{v_n^2\}$, $\hat{\mathbf{x}}_n^- \doteq \hat{E}\{\mathbf{x}_n|y_{n-1}, ..., y_1\}$ is the *a priori* estimate of the state vector $\mathbf{x}_n$ in the n^{th} stage using the observations y_1 to y_{n-1}, and $\hat{\mathbf{x}}_n^+ \doteq \hat{E}\{\mathbf{x}_n|y_n, ..., y_1\}$ is the *a posteriori* estimate of this state vector after using the n^{th} observation y_n. The matrices P_n^- and P_n^+ are defined in the same manner to be the *a priori* and *a posteriori* estimates of the state vector covariance matrices before and after using the n^{th} observation, respectively. Finally, $\mathbf{K}_n$ is the Kalman filter gain.

It is seen from (5)-(8) that the amplitude and phase of the PLI defined in (1), do not appear in the dynamic model of the system. This means that they do not affect the filter convergence and the filter will implicitly estimate their values.

Note that although we run the proposed KF to estimate $\hat{x}_n$ (the PLI), in PLI cancellation we are finally interested in the *innovation* signal of the KF, i.e.,

$$\hat{v}_n = y_n - \hat{x}_n^-, \tag{9}$$

which represents the PLI-removed signal of interest.

III. Stability and Convergence

The proposed dynamic model is only *marginally stable*, since the eigenvalues of the matrix A are $\lambda(A) = e^{\pm j\omega_0}$, which exactly lie on the unit circle. This is apparently due to the oscillatory nature of the PLI. However, since the rank of the *controllability matrix* $R_c \doteq [\mathbf{b} \quad A\mathbf{b}]$ and the *observability matrix* $R_o \doteq [\mathbf{h} \quad A^T\mathbf{h}]$ is equal to two, i.e., equal to the state vector dimensions, the system is both *controllable* and *observable* [15]. This practically means that despite the marginal stability of the model, the PLI may indeed be estimated by this KF and the filter converges to its final value, i.e., the value with the least minimum mean square error, in finite time from any initial state. This result is theoretically justified in the appendix with another approach.

In the context of estimation theory, it is proved that for stationary processes, a stable KF converges to the optimal *Wiener filter* in steady state. The time of convergence depends on the covariances of the model and observation noises, namely q_n and r_n (or merelly to their ratio, as we will later show). This steady state behavior is studied in the following section.

It should be noted that some of the properties of the KF, such as optimality, are only literally achieved under the assumptions of stationary white Gaussian signals. In our developed framework, the KF considers the desired biosignals as noise for the PLI, and these signals are not necessarily Gaussian and the noise covariance r_n is generally a function of time. Nevertheless, as we will show in the results, a good choice of the filter parameters results in very robust results.

IV. Steady State Analysis

It is insightful to study the characteristics of the proposed filter in steady state for stationary process models ($q_n = q$) and stationary observations ($r_n = r$). To do so, we adopt a frequency domain approach (cf. [17, Ch. 4]). First of all, by combining (6) and (8), the posterior Kalman state estimate $\hat{\mathbf{x}}_n^+$ may be rewritten as follows:

$$\hat{\mathbf{x}}_n^+ = (I - \mathbf{K}_n\mathbf{h}^T)A\hat{\mathbf{x}}_{n-1} + \mathbf{K}_n y_n \tag{10}$$

[1] The zero-mean assumption does not confine the generality of the model.

[2] In the context of control theory, *controllability* is a property of a system, describing the ability to drive the system states to arbitrary values through the input signal or noise in finite time. Its dual notion of *observability* describes the ability to infer the system states given output measurements [15], [16].

Assuming that the filter has reached its steady state, following the discussions of Section III, the Kalman gain converges to a constant value $\bar{\mathbf{K}} \doteq \lim_{n\to\infty} \mathbf{K}_n = [k_1 \quad k_2]^T$. In the appendix, it is shown that $\bar{\mathbf{K}}$ is found by solving the well-known *discrete algebraic Ricatti equation* (DARE), as follows:

$$\bar{\mathbf{K}} = \begin{bmatrix} k_1 \\ k_2 \end{bmatrix} = \begin{bmatrix} \dfrac{\tilde{p}}{\tilde{p}+1} \\ \dfrac{2\tilde{p}\cos(\omega_0)}{(\tilde{p}+1)(\tilde{p}+2)} \end{bmatrix} \tag{11}$$

where $\tilde{p}$ is a constant parameter found by solving DARE as a function of the ratio $\gamma = q/r$. Therefore, in steady state, (10) reduces to:

$$\hat{\mathbf{x}}_n^+ = (I - \bar{\mathbf{K}}\mathbf{h}^T)A\hat{\mathbf{x}}_{n-1} + \bar{\mathbf{K}}y_n \tag{12}$$

Taking the Z-transform of (12), yields:

$$\mathbf{H}(z) \doteq \hat{\mathbf{X}}(z)^+/Y(z) = [I - (I - \bar{\mathbf{K}}\mathbf{h}^T)Az^{-1}]^{-1}\bar{\mathbf{K}} \tag{13}$$

where $\mathbf{H}(z)$ represents the transfer vector of the KF in its steady state. $\mathbf{H}(z)$ is a filter that takes the observations y_n as its input and gives $\hat{\mathbf{x}}_n^+$ in the output. This filter is known as a *state observer* in the context of control theory. In order to calculate $\mathbf{H}(z)$, we insert the values of matrices A and $\bar{\mathbf{K}}$ in (13). After some algebraic simplifications, we find:

$$\mathbf{H}(z) \doteq \begin{bmatrix} H_1(z) \\ H_2(z) \end{bmatrix} = \begin{bmatrix} \dfrac{k_1 - k_2 z^{-1}}{1 - [k_2 + 2(1-k_1)\cos(\omega_0)]z^{-1} + (1-k_1)z^{-2}} \\ \dfrac{k_2 + [k_1 - 2\cos(\omega_0)k_2]z^{-1}}{1 - [k_2 + 2(1-k_1)\cos(\omega_0)]z^{-1} + (1-k_1)z^{-2}} \end{bmatrix} \tag{14}$$

Recalling the definition of the state vector $\mathbf{x}_n = [x_n \quad x_{n-1}]^T$, we are specifically interested in the first entry of $\mathbf{H}(z)$, which is the filter that estimates x_n (the PLI) from the noisy observations y_n. Moreover, from (9) it is known that we are ultimately interested in finding the PLI-removed biosignals. Therefore, the overall transfer function of interest, i.e., the filter that removes the PLI from the noisy biosignal, is

$$G(z) \doteq \frac{\hat{V}(z)}{Y(z)} = 1 - H_1(z) \tag{15}$$

Inserting (11) in (14) and (15), yields the final result:

$$G(z) = \alpha \frac{1 - 2\cos(\omega_0)z^{-1} + z^{-2}}{1 - \cos(\omega_0)\left(\dfrac{4\alpha}{\alpha+1}\right)z^{-1} + \alpha z^{-2}}, \tag{16}$$

where $\alpha = 1/(\tilde{p}+1)$. It is seen that the transfer function is very close to standard second order digital notch filters[3] [2],

[3]We recall that a digital notch filter obtained from *bilinear transformation* of a second order analog notch filter has the following form:

$$G(z) = (\frac{1+\alpha}{2})\frac{1 - 2\cos(\omega_0)z^{-1} + z^{-2}}{1 - \cos(\omega_0)(1+\alpha)z^{-1} + \alpha z^{-2}},$$

where $\alpha = \dfrac{1 - tan(\mathrm{BW}/2)}{1 + tan(\mathrm{BW}/2)}$ and BW is the -3dB bandwidth; cf. [18, p. 434].

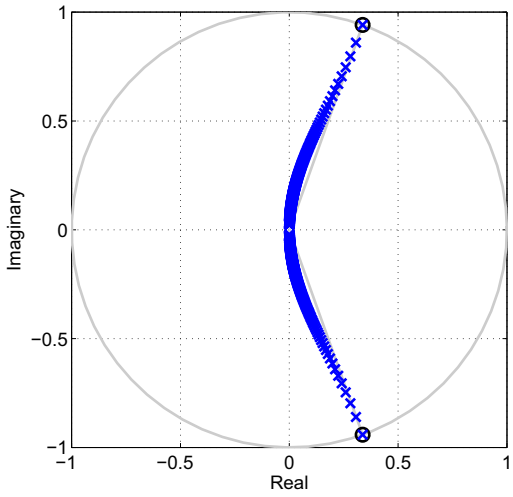

Fig. 1. The root loci of the designed KF in steady state subject to variations of the parameter $\tilde{p}$, for f_0=50Hz and f_s=256Hz. The filter has two fixed conjugate zeros on the unit circle and two conjugate poles that approach the origin as $\tilde{p} \to \infty$. Notice the minor deviation of the poles from the streight line between the zeros and the origin.

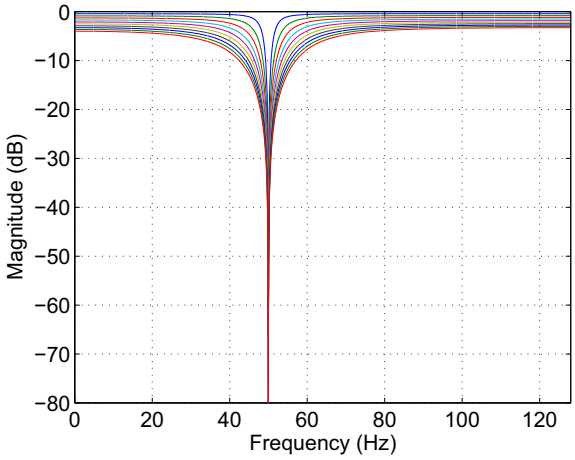

Fig. 2. The KF response in steady state with variation of the parameter $\tilde{p}$ from 0.1 to 1 in 0.1 steps (from top to bottom), for f_0=50Hz and f_s=256Hz.

[3]. The root locus of this transfer function is depicted in Fig. 1, for f_0=50Hz and f_s=256Hz. Accordingly, the filter has two conjugate zeros on the unit circle at $z = e^{\pm j\omega_0}$, which produce the notch in the filter's spectrum, and two conjugate poles inside the unit circle, which for small values of $\tilde{p}$ are almost on the same axis as the two zeros. These poles deviate from the axis of the zeros for large values of $\tilde{p}$ and approach the origin of the complex plane as $\tilde{p} \to \infty$. Note that although the pole-zero configurations vary with the ratio f_0/f_s, the hereby stated general structure is preserved. The frequency responses of different filters obtained by varying $\tilde{p}$ are depicted in Fig. 2. It is seen that the Q-factor of the notch filter changes with $\tilde{p}$. As noted before, the tunable parameters of the filter are q and r. More precicely, as shown in the appendix (cf. (25)),

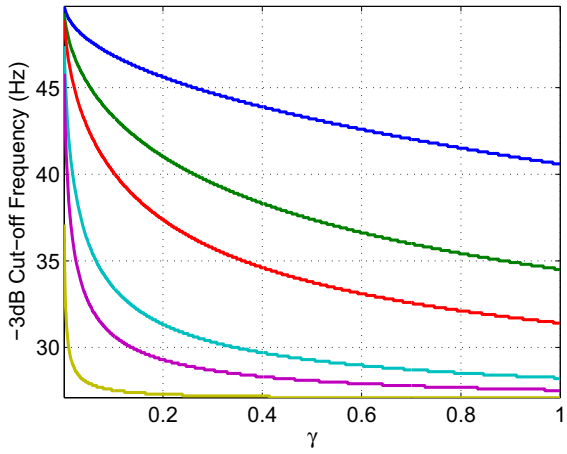

Fig. 3. The KF -3dB cut-off frequency versus γ for f_0=50Hz and f_s=128Hz, 200Hz, 256Hz, 400Hz, 512Hz, and 1000Hz (from top to bottom).

by fixing the notch frequency ratio at f_0/f_s, the only tunable parameter of the algorithm is $\gamma = q/r$, which alters $\tilde{p}$ and the filter's Q-factor. In Fig. 3, the explicit relation between γ and the filter's -3dB cut-off frequency is shown for f_0=50Hz and various sampling frequencies f_s that are typical in biomedical applications. Note that only the ratio of f_0/f_s effects the filter response. Therefore, the curves are simply extendable for f_0=60Hz and other sampling frequencies.

It should also be noted that the filter in (16) slightly attenuates the signals in its pass-band (DC gain $<$ 0dB). As we can see in Fig. 2 this attenuation increases with $\tilde{p}$ (or equivalently γ). The DC offset of the filter can be directly calculated from (16) and be corrected in the filter's output in case of necessity.

To summarize we have shown that in steady state, the proposed KF is merely a second order notch filter that adapts its Q-factor according to the signal/noise contents ($\gamma = q/r$) of the noisy signal (cf. [2], [3]). Moreover, as a Kalman filter, it is an optimal linear filter (in the minimum mean square error sense), and is guaranteed to be stable.

V. Implementation Issues

The online update of the filter parameters is indeed important. Otherwise, following the discussions in Section IV, the filter simply converges to an approximate second order notch filter.

As noted before, for a fixed notch frequency ratio f_0/f_s, the only tunable parameter of the proposed filter is $\gamma_n = q_n/r_n$ (or γ in steady state). The parameter r_n can be found by passing the observations through a coarse fixed-bandwidth notch filter and calculating the variance of the resulting signal, which is a reasonable estimate of the non-PLI signal variance. On the other hand, if the range of amplitude, phase, or frequency deviations of the dynamic model are known (from *a priori* information about the observed data), one can derive the variance of the model error q_n. Having r_n and q_n, γ_n is simply calculated.

Alternatively, a more practical approach for modifying γ_n is to choose an average value for it, say, $\bar{\gamma}$. According to the results in Fig. 3, $\bar{\gamma}$ is related to the average Q-factor or equivalently the average -3dB cut-off frequency of the filter. Next, γ_n can be tuned according to the signal/noise variations of the signal to automatically adapt its Q-factor around $\bar{\gamma}$. This idea can be implemented in various ways. We adopt a method based on the innovation signal. As proposed in [12], [19], at time instant k, we define

$$\mu_k = \frac{1}{L} \sum_{n=k-L+1}^{k} \frac{\hat{v}_n^2}{\mathbf{h}^T P_n^- \mathbf{h} + r_n} \tag{17}$$

where $\hat{v}_n$ is the innovation signal of the KF defined in (9) and L is the length of a moving average window. The denominator of μ_k is merely the KF estimated variance of $\hat{v}_n$, i.e., $E\{\hat{v}_n^2\}$. In fact, μ_k is an average of the variances of the L recent innovations, normalized by their KF estimated values. Therefore, as long as the KF is functioning correctly, $\mu_k \approx 1$. Values of μ_k much greater than unity indicate that the innovation signal variance is being underestimated by the KF, while values close to zero indicate that the innovation signal variance is being overestimated. μ_k is a dimensionless parameter that can be used to alter $\bar{\gamma}$:

$$\gamma_k = \mu_k \cdot \bar{\gamma} \tag{18}$$

Other ideas for adaptation of the filter parameters have been studied in [20].

VI. Multiple Harmonics

It is straightforward to extend the proposed filtering framework to multiple notch frequencies or harmonics. One approach is to use the proposed filter in multiple stages; with each stage designed for removing one of the harmonics of interest. Specifically, for the third and fifth harmonics of the PLI, since the harmonics are well-spaced in the frequency domain, each filter will only effect its corresponding notch frequency. A second approach is to model each of the harmonics with a separate model, identical to (3), and to augment their corresponding state equations within a single dynamical model. In this case, the observed signals can be considered as a superposition of the harmonics and other signals. The dynamic equations leading to the multiple harmonic extension is

$$\begin{aligned} x_{n+1}^1 + x_{n-1}^1 &= 2\cos(\omega_1) x_n^1 + w_n^1 \\ x_{n+1}^2 + x_{n-1}^2 &= 2\cos(\omega_2) x_n^2 + w_n^2 \\ &\cdots \\ x_{n+1}^N + x_{n-1}^N &= 2\cos(\omega_N) x_n^N + w_n^N \\ y_n &= x_n^1 + x_n^2 + \cdots + x_n^N + v_n, \end{aligned} \tag{19}$$

where x_n^i $(i = 1, \cdots, N)$ are the state variables used for modeling each of the N harmonics $\omega_i = 2\pi f_i/f_s$. Note that, as before, the amplitudes and phases of the harmonics do not appear in the dynamic equations and are not required in the filtering procedure.

The study of the steady state behavior of this extension is rather lengthy and beyond the scopes of this paper. However,

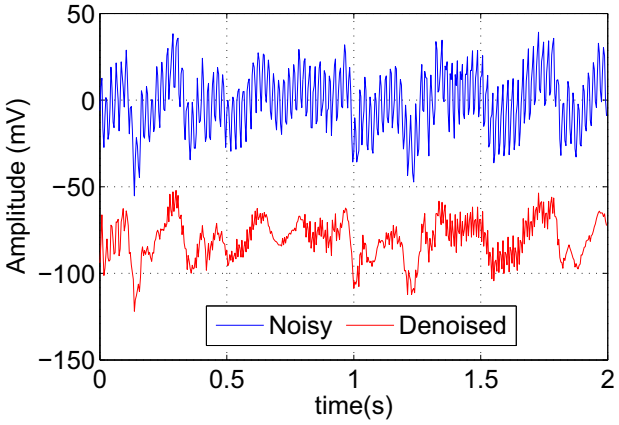

Fig. 4. A segment of noisy (top) and denoised (bottom) EEG signals

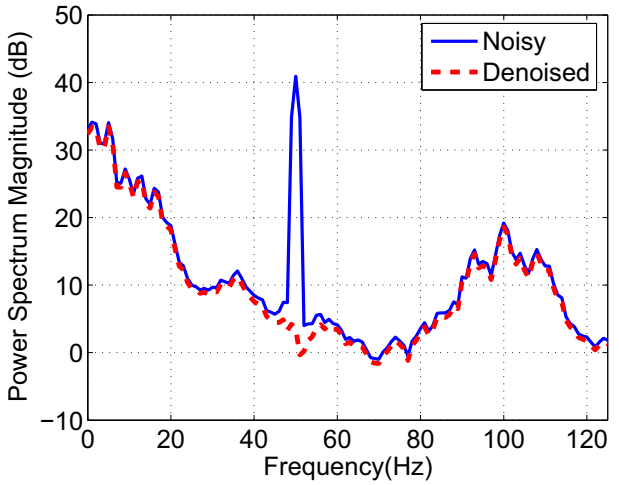

Fig. 5. Comparison of the EEG signal spectra before and after denoising

due to the decoupled state variables of this model and the block diagonal structure of its resulting matrix form, it is straightforward to derive the dynamic equations of this filter.

VII. Case Studies

The proposed filter has been implemented in Matlab®.Our first case study concerns real electroencephalogram (EEG) signals diluted by PLI. The corresponding EEG signals before and after denoising and their corresponding spectra are shown in Figs. 4 and 5. It is seen that the original EEG is highly contaminated by PLI and the EEG waveforms are totally masked by the PLI. This noise has been effectively suppressed by the proposed filter. The parameters for this example were f_s=250Hz, f_0=50Hz, $\bar{\gamma}$=10^{-4} and L=25. As a second example, in Fig. 6, PLI has been synthetically generated and added to clean electrocardiogram (ECG) signals and the proposed filter results are compared with the original and noisy ECG. The PLI amplitude was modulated with a 0.2 Hz sinusoid to represent respiratory coupled changes in the PLI amplitude. The result of a classical second-order IIR notch filter with a Q-factor of 50 is also depicted for comparison. In this study f_s=1000Hz,

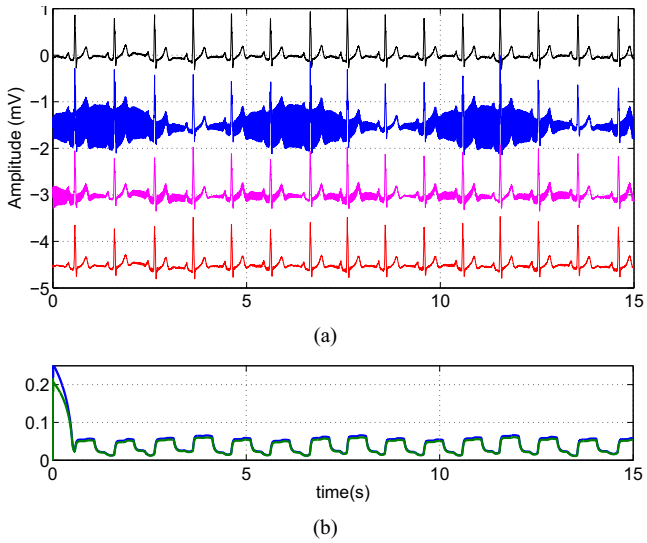

Fig. 6. (a) From top to bottom: a segment of original ECG, diluted, denoised using a second-order notch IIR filter, and denoised using the proposed method (b) The Kalman Gain vector $\mathbf{K}_n$ (the two entries of $\mathbf{K}_n$ are plotted over one another)

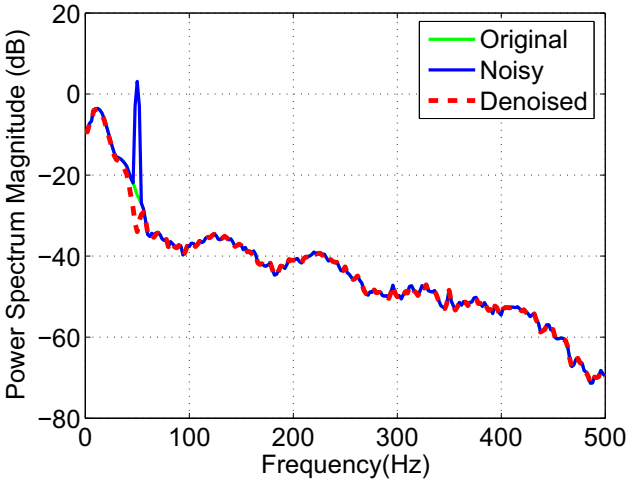

Fig. 7. Comparison of the ECG signal spectra before and after denoising using the proposed Kalman filter

f_0=50Hz, $\bar{\gamma}$=0.01 and L=1000 (i.e., the averaging window length defined in (17) is 1s). From Fig. 6 is can be seen that the proposed filter has successfully followed the original ECG, while the classical notch filter is susceptible to the amplitude changes of the PLI (i.e. nonstationarity of the PLI). Note that a decrease in the IIR notch filter's Q-factor improves the results of this filter, but it will also remove some ECG components.

The spectra of the data before and after PLI cancellation are shown in Fig. 7, where the performance of the filter is clearly seen. Note that comparing the parameters of this example with the previous example, the greater value of $\bar{\gamma}$ is due to the smaller sampling frequency of EEG signals as compared with the ECG (cf. Fig. 3).

VIII. Conclusion

In this paper a discrete-time linear Kalman notch filter was presented for removing power-line interference from noisy biosignals.

As compared to conventional notch filters and active noise cancelers, the novelty of the hereby proposed technique was to formulate the dynamics of a sinusoid in a simple linear form, which only depends on the sinusoidal frequency, and to use this model within a linear Kalman filtering framework. The theoretical details and performance of the proposed method were studied in details and two case studies were presented for EEG and ECG denoising. It was shown that in steady state the proposed filter performs rather similar to conventional active noise cancelers. In this work, no special assumptions were made about the temporal dynamics of the biosignals contaminated by PLI. However, in future works, if any information is available about the dynamics of these signals, the presented technique can be *state augmented* with the signal dynamics, to form a general framework for biosignal denoising. It was also shown that the extension of this technique to multiple notch frequencies is rather simple and straightforward, an issue that may be of interest in many practical applications.

Appendix
Solution of the Ricatti Equation

Following the discussions of Section IV, in steady state, the covariance matrices and the Kalman gain defined in (6)-(8), converge to constant values

$$\begin{aligned} \bar{\mathbf{K}} &\doteq \lim_{n\to\infty} \mathbf{K}_n = [k_1 \quad k_2]^T, \\ \bar{P} &\doteq \lim_{n\to\infty} P_n^- = \begin{bmatrix} p_1 & p_2 \\ p_3 & p_4 \end{bmatrix} \end{aligned} \tag{20}$$

that may be calculated by solving the nonlinear *discrete algebraic Ricatti equation* (DARE) [17], [21]:

$$\bar{P} = A\bar{P}A^T - \frac{A\bar{P}\mathbf{h}\mathbf{h}^T\bar{P}A^T}{\mathbf{h}^T\bar{P}\mathbf{h} + r} + q\mathbf{b}\mathbf{b}^T \tag{21}$$

By direct algebraic calculations, it can be shown that

$$\bar{\mathbf{K}} = [\frac{p_1}{p_1 + r} \quad \frac{p_3}{p_1 + r}]^T, \tag{22}$$

and

$$\begin{aligned} p_4 &= \frac{p_1 r}{p_1 + r}, \quad p_2 = p_3 = \frac{2rp_1\cos(\omega_0)}{p_1 + 2r}, \\ p_1 &= \frac{4rp_1\cos(\omega_0)^2 - 4rp_2\cos(\omega_0) + \det(\bar{P}) + rp_4}{p_1 + r} + q \end{aligned} \tag{23}$$

To solve these equations, we replace p_2, p_3, and p_4 in the last equation of (23), which results in

$$\frac{p_1^2}{p_1 + r} = \frac{4rp_1^2\cos(\omega_0)^2}{(p_1 + 2r)^2} + q \tag{24}$$

To simplify the notations we define the normalized parameters $\tilde{p} \doteq p_1/r$, $\gamma \doteq q/r$ and $\tilde{P} = \bar{P}/r$. Using these definitions, (24) reduces to

$$\frac{\tilde{p}^2}{\tilde{p} + 1} = \frac{4\tilde{p}_1^2\cos(\omega_0)^2}{(\tilde{p} + 2)^2} + \gamma \tag{25}$$

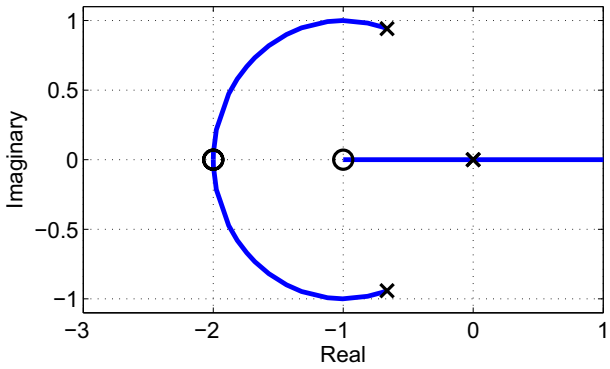

Fig. 8. The root locus of $\tilde{p}$ found from DARE, for $0 \leq \gamma < \infty$. Notice its one and only real non-negative solution on the right part of the real axis.

or, equivalently,

$$\tilde{p}^4 + [4\sin(\omega_0)^2 - \gamma]\tilde{p}^3 + [4\sin(\omega_0)^2 - 5\gamma]\tilde{p}^2 - 8\gamma\tilde{p} = 4\gamma \tag{26}$$

As we can see, for a fixed value of ω_0, the solution of this equation is only a function of γ. By transforming it into the following form, one can visualize the location of its solutions by classical root locus methods

$$1 - \gamma\frac{(\tilde{p} + 1)(\tilde{p} + 2)^2}{\tilde{p}^2(\tilde{p} + 1 - e^{j2\omega_0})(\tilde{p} + 1 - e^{-j2\omega_0})} = 0 \tag{27}$$

The root locus of $\tilde{p}$ subject to the variations of γ is shown in Fig. 8, for f_0=50Hz and f_s=256Hz; where it is seen that one and only one of the roots of this equation is always real and positive (cf. [21, P. 22 and Appendix E]). Moreover, this result is general and does not depend on the notch frequency and the sampling rate. The overall effect of the parameter γ on the -3dB cut-off frequency of the filter's notch frequency was previously shown in Fig. 3.

It is also interesting to note that comparing (23) and (24) and using the normalized parameters defined above, we arrive at:

$$\det(\tilde{P}) = \gamma \geq 0 \tag{28}$$

which is the product of eigenvalues of $\tilde{P}$ and may be interpreted as the area enclosed by the trajectories of the state vector $\mathbf{x}_n^-$ in steady state. This result, together with the existence of a non-negative solution for $\tilde{p}$, yields the positive definiteness of the solution $\tilde{P}$, which proves the convergence and stability of the proposed filter [22, Ch. 7, P. 197].

References

[1] A. Nehorai, "A minimal parameter adaptive notch filter with constrained poles and zeros," *Acoustics, Speech and Signal Processing, IEEE Transactions on*, vol. 33, no. 4, pp. 983 – 996, aug 1985.

[2] B. Widrow, J. Glover, J. McCool, J. Kaunitz, C. Williams, H. Hearn, J. Zeidler, E. Dong, and R. Goodlin, "Adaptive Noise Cancelling: Principles and Applications," *Proc. IEEE*, vol. 63, no. 12, pp. 1692–1716, 1975.

[3] J. Glover, J., "Adaptive Noise Canceling Applied to Sinusoidal Interferences," *Acoustics, Speech and Signal Processing, IEEE Transactions on*, vol. 25, no. 6, pp. 484 – 491, dec 1977.

[4] P. Tichavsky and A. Nehorai, "Comparative study of four adaptive frequency trackers," *Signal Processing, IEEE Transactions on*, vol. 45, no. 6, pp. 1473 –1484, jun 1997.
[5] M. Sedlacek and J. Blaska, "Low uncertainty power-line frequency estimation for distorted and noisy harmonic signals," *Measurement*, vol. 35, no. 1, pp. 97 – 107, 2004. [Online]. Available: http://www.sciencedirect.com/science/article/pii/S0263224103000952
[6] M. Dragosevic and S. Stankovic, "An adaptive notch filter with improved tracking properties," *Signal Processing, IEEE Transactions on*, vol. 43, no. 9, pp. 2068 –2078, sep 1995.
[7] P. Dash, R. Jena, G. Panda, and A. Routray, "An extended complex kalman filter for frequency measurement of distorted signals," *Instrumentation and Measurement, IEEE Transactions on*, vol. 49, no. 4, pp. 746 –753, aug 2000.
[8] A. Routray, A. Pradhan, and K. Rao, "A novel kalman filter for frequency estimation of distorted signals in power systems," *Instrumentation and Measurement, IEEE Transactions on*, vol. 51, no. 3, pp. 469 –479, jun 2002.
[9] L. D. Avendaño-Valencia, L. E. Avendaño, J. Ferrero, and C. G. Castellanos-Domínguez, "Improvement of an extended kalman filter power line interference suppressor for ECG signals," in *Computers in Cardiology, 2007*, 30 2007-oct. 3 2007, pp. 553 –556.
[10] L. D. Avendaño-Valencia, L. E. Avendaño, C. G. Castellanos-Domínguez, and E. J. Villegas-Jaramillo, "Reduction of power line interference on ecg signals using kalman filtering and delta operator," 2007.
[11] D. G. Fink and H. W. Beaty, *Standard Handbook for Electrical Engineers,, 1978, ISBN 0-07-020974-X, page 16-15, 16-16*, 15th ed. McGraw-Hill, 2006.
[12] R. Sameni, M. B. Shamsollahi, C. Jutten, and G. D. Clifford, "A Nonlinear Bayesian Filtering Framework for ECG Denoising," *IEEE Trans. Biomed. Eng.*, vol. 54, no. 12, pp. 2172–2185, December 2007.
[13] R. Sameni, M. B. Shamsollahi, and C. Jutten, "Model-based Bayesian filtering of cardiac contaminants from biomedical recordings," *Physiological Measurement*, vol. 29, no. 5, pp. 595–613, May 2008.
[14] J. van Zaen, L. Uldry, C. Duchêne, Y. Prudat, R. A. Meuli, M. M. Murray, and J.-M. Vesin, "Adaptive tracking of EEG oscillations," *Journal of Neuroscience Methods*, vol. 186, no. 1, pp. 97–106, 2010.
[15] T. Kailath, *Linear Systems*. Prentice Hall, 1980.
[16] K. S. Tsakalis, "Stability, controllability, observability," June 2001, Lecture Notes. [Online]. Available: http://tsakalis.faculty.asu.edu/notes/sco.pdf
[17] B. D. O. Anderson and J. B. Moore, *Optimal Filtering*. Dover Publications, Inc., 1979.
[18] S. K. Mitra, *Digital Signal Processing: A Computer Based Approach*, 3rd ed. McGraw-Hill, 2005.
[19] M. A. Maasoumnia, "Estimation Theory and Optimal Filtering, [Lecture Notes]," 2003, Sharif University of Technology, Tehran, Iran.
[20] M. P. Tarvainen, S. D. Georgiadis, P. O. Ranta-aho, and P. A. Karjalainen, "Time-varying analysis of heart rate variability signals with a Kalman smoother algorithm," *Physiol. Meas.*, vol. 27, pp. 225–239, Mar. 2006.
[21] T. Kailath, A. H. Sayed, and B. Hassibi, *Linear Estimation*. Prentice Hall, 2000.
[22] D. Simon, *Optimal State Estimation: Kalman, H Infinity, and Nonlinear Approaches*. John Wiley & Sons Inc., 2006.